Published in final edited form as:
J Comp Neurol. 2011 June 1; 519(8): 1455–1475. doi:10.1002/cne.22576.

Synaptic Proteins Are Tonotopically Graded in Postnatal and Adult Type I and Type II Spiral Ganglion Neurons

Jacqueline Flores-Otero and **Robin L. Davis***
Department of Cell Biology and Neuroscience, Rutgers University, Piscataway, New Jersey 08854

Abstract

Inherent in the design of the mammalian auditory system is the precision necessary to transduce complex sounds and transmit the resulting electrical signals to higher neural centers. Unique specializations in the organ of Corti are required to make this conversion, such that mechanical and electrical properties of hair cell receptors are tailored to their specific role in signal coding. Electrophysiological and immunocytochemical characterizations have shown that this principle also applies to neurons of the spiral ganglion, as evidenced by distinctly different firing features and synaptic protein distributions of neurons that innervate high- and low-frequency regions of the cochlea. However, understanding the fine structure of how these properties are distributed along the cochlear partition and within the type I and type II classes of spiral ganglion neurons is necessary to appreciate their functional significance fully. To address this issue, we assessed the localization of the postsynaptic AMPA receptor subunits GluR2 and GluR3 and the presynaptic protein synaptophysin by using immunocytochemical labeling in both postnatal and adult tissue. We report that these presynaptic and postsynaptic proteins are distributed oppositely in relation to the tonotopic map and that they are equally distributed in each neuronal class, thus having an overall gradation from one end of the cochlea to the other. For synaptophysin, an additional layer of heterogeneity was superimposed orthogonal to the tonotopic axis. The highest anti-synaptophysin antibody levels were observed within neurons located close to the scala tympani compared with those located close to the scala vestibuli. Furthermore, we noted that the protein distribution patterns observed in postnatal preparations were largely retained in adult tissue sections, indicating that these features characterize spiral ganglion neurons in the fully developed ear.

Keywords

NT-3; BDNF; synaptic proteins; spiral ganglion; auditory nerve

Extracting modality-specific information from complex sensory stimuli begins with specializations that have been well characterized within many different types of sensory receptors. These specializations are not limited to the sensory end organs, but there is evidence that they are also present within primary afferents (Loewenstein and Mendelson, 1965; Scroggs and Fox, 1992; Scroggs et al., 1994; Yamagata et al., 2006). Nowhere are the afferents more strictly organized, however, than in the peripheral auditory ganglion,

*CORRESPONDENCE TO: Dr. Robin L. Davis, Department of Cell Biology and Neuroscience, 604 Allison Road, Nelson Laboratories, Rutgers University, Piscataway, NJ 08854. rldavis@rci.rutgers.edu.

Additional Supporting Information may be found in the online version of this article.

affording the opportunity to examine how their phenotypic organization contributes to the initial stages of sensory coding.

The peripheral auditory system constructs a primary map of frequency by decomposing sound into its component parts, utilizing a wealth of mechanical and cellular specializations (Rubel and Fritzsch, 2002; Raphael and Altschuler, 2003). Also specialized is the first neural element, the spiral ganglion neurons. From the subtle changes in their electrophysiological features and the related composition of voltage-gated ion channels (Adamson et al., 2002b), to the enrichment of synaptically related proteins (Flores-Otero et al., 2007), the tonotopic relevance is beginning to be revealed. Moreover, neurotrophins that have been found to regulate these electrophysiological features (Adamson et al., 2002a; Zhou et al., 2005; Flores-Otero et al., 2007), brain-derived neurotrophic factor (BDNF) and neurotrophin-3 (NT-3), show tonotopic gradients in their distribution. BDNF is graded within the ganglion neurons themselves such that the highest levels were found in the base (Schimmang et al., 2003), whereas NT-3 promoter expression is graded in the opposite direction; the highest levels are observed in the apex in newborn (Fritzsch et al., 1997), postnatal, and adult cochleae (Sugawara et al., 2007).

In vitro analysis of the firing features of type I spiral ganglion neurons have shown that ion channels associated with rapid responsiveness to abrupt changes in voltage were preferentially localized to cells within the high-frequency region of the ganglion, whereas neurons with slower response properties were located in the low-frequency region of the ganglion (Adamson et al., 2002b). Systematic changes in the ion channel composition and electrophysiological features that represent timing information form a gradient that coincides with the tonotopic organization within the cochlea (Adamson et al., 2002b; Liu and Davis, 2007). This correspondence was limited to parameters that contributed to timing-related electrical features. Neuronal thresholds, for example, were distributed nonmonotonically, such that the most excitable neurons were located within the midfrequency region of the ganglion (Liu and Davis, 2007). For all parameters measured, it is also important to note that local heterogeneity was characteristic of all cochlear regions. Therefore, based solely on the distribution pattern of these features, different predictions regarding their function could be made. In the case of electrical characteristics that convey timing-related features, one would expect that they contribute to the frequency-dependent coding requirements of the system, whereas, for the case of threshold levels, in which the most excitable neurons reside within the midfrequency region, one would expect that these properties are tailored to the sensitivity requirements of the system.

In addition to graded levels of proteins that regulate neuronal firing, amounts of synaptic proteins also varied along the cochlear partition. Work from our laboratory has shown that synaptic proteins were distributed differentially in postnatal spiral ganglion neurons innervating high- and low-frequency regions (Flores-Otero et al., 2007). High-frequency neurons were enriched for postsynaptic AMPAR subunits GluR2 and GluR3 yet showed low levels of presynaptic synaptophysin and SNAP-25. In contrast, immunocytochemical observations from low-frequency neurons were consistent with low AMPAR protein levels but high synaptophysin and SNAP-25 protein levels. Issues not addressed in previous work, however, are whether the distribution of these proteins was graded or discrete, whether the tonotopic distributions were present in postnatal and adult spiral ganglion neuronal tissues and acute preparations, and whether differences in synaptic proteins also applies to type II neurons. As has already been seen for the intrinsic electrical properties of the neurons, information regarding the basic distribution patterns of synaptic proteins will undoubtedly yield important insights into their functional significance.

Therefore, studies were undertaken to examine the frequency specificity of the synaptic protein localization patterns in both classes of spiral ganglion neuron. We found by immunocytochemical analysis that both the presynaptic and the postsynaptic protein distributions were relatively similar for type I and II neurons, each exhibiting evidence of a graded pattern across the cochlear partition. Synaptophysin was progressively enriched in apical type I and II neurons, whereas GluR2/3 levels showed the opposite progression, being highest in basal neurons. These gradients were found both in postnatal and in adult cochleae, indicating that their functional significance must be considered within the framework of the mature organ. Furthermore, by evaluating local synaptophysin heterogeneity in postnatal tissues, we discovered an additional gradient distributed orthogonal to the tonotopic axis. This distribution is comparable to previous observations of spontaneous rate classes (Leake et al., 1992) and indicates that neuronal “hypercolumns” may exist within the spiral ganglion.

MATERIALS AND METHODS

Tissue culture

Procedures performed on CBA/CaJ mice were approved by the Rutgers University Institutional Review Board for the Use and Care of Animals (IRB-UCA), protocol 90-073. CBA/CaJ mice were decapitated, and both inner ears were removed from the base of the cranium. Spiral ganglia were isolated from postnatal day 6–7 (PD 6–7) animals and divided into thirds; base and apex sections were plated as explants in culture dishes coated with poly-L-lysine. Cells were maintained in growth medium: Dulbecco's modified Eagle's medium (DMEM), supplemented with 10% fetal bovine serum, 4 mM L-glutamine, and 0.1% penicillin-streptomycin. Neurons were maintained in culture for 6 days at 37°C in a humidified incubator with 5% CO_2.

Paraffin-embedded sections

Cochlear sections were obtained from PD 5–7 and adult (6–8 months) CBA/CaJ mice. Adult animals were anesthetized by intraperitoneal injection with 250 mg/kg avertin and perfused intracardially first with 0.01 M PBS (pH 7.4) and subsequently with 10% formalin or 100% methanol fixative. Mice were decapitated, and temporal bones were removed, rinsed overnight in 0.01 M PBS at RT, and decalcified in 0.12 M ethylenediaminetetraacetic acid (EDTA; pH 7.2) for 5 days at RT; EDTA was changed every 24 hours. Postnatal animals were decapitated, and temporal bones were removed and placed in either 10% formalin or 100% methanol for 45 minutes, followed by three rinses with 0.01 M PBS (pH 7.4) for 15 minutes each or overnight at RT. Adult and postnatal temporal bones were dehydrated in 50%, 75%, 80%, and 95% ethanol for 1 hour each, followed by 95% ethanol for an additional 1 hour, 100% ethanol for 30 minutes, and n-butanol overnight at RT. On the next day, n-butanol was replaced with fresh n-butanol, which was applied for an additional 2 hours. Finally, temporal bones were embedded in paraffin, sectioned at 4–6 μm thickness, placed on poly-L-lysine-coated glass slides (VWR; 48311-703), dried overnight, and stored at RT until ready for use.

Immunocytochemistry

Paraffin-embedded sections—Cochlear sections containing two to four neuronal groups were selected for immunolabeling of spiral ganglion neurons or sensory hair cells. Before the staining procedure, sections were dewaxed in Histoclear (National Diagnostics; HS-200) for 10 minutes and rehydrated twice for 5 minutes at RT in 100%, 95%, 85%, 75%, 50% ethanol and ddH_2O. Double immunofluorescence staining consisted of blocking with 5% normal goat serum (NGS) for 1 hour, primary antibody application (either 1 hour at RT or 24–48 hours at 4°C), followed by incubation with a conjugated secondary antibody (1

hour at RT at 1:100 dilution). After the application of primary and secondary antibodies, sections were rinsed three times with 0.01 M PBS. Sections were covered with Dabco, coverslipped, and viewed immediately.

Adult sections were autofluorescent and therefore were stained with the avidin biotinylated enzyme complex technique (Vectastain ABC Systems; Vector, Burlingame, CA). Subsequent to rehydration, adult sections were blocked with the appropriate blocking serum from the ABC kit (1 hour at RT). To block endogenous biotin, sections were then treated with avidin D blocking solution for 15 minutes; then, a brief rinse with 0.01 M PBS was performed, and biotin blocking solution was applied for 15 minutes. Primary antibody was then applied either for 24 or 48 hours at 4°C, and sections were subsequently incubated with a biotinylated secondary antibody (1 hour at RT; 1:100 dilution). After the application of primary and secondary antibodies, sections were rinsed three times with 0.01 M PBS. The Vectastain Elite ABC reagent was applied to each section for 30 minutes in a covered chamber, followed by three rinses with 0.01 M PBS. To amplify the signal, adult sections were incubated with biotinyl tyramide (BT) amplification reagent for 5 minutes. Sections were then rinsed three times with 0.01 M PBS and reincubated for 30 minutes with the Vectastain Elite ABC reagent. After three washes with 0.01 M PBS, the 3,3′-diaminobenzidine (DAB) substrate enhancing solution was applied to sections for ~1–4 seconds, after which sections were rinsed twice with ddH_2O for 5 minutes each. Sections were then dehydrated for 5 minutes in 50%, 75%, 85%, 95% and twice in 100% ethanol. These were then placed twice in Histoclear (10 minutes each). Finally, sections were covered with Vectamount, coverslipped, and stored at RT until dried.

In vitro preparations—Double immunofluorescence of spiral ganglion neurons was performed on cultures that had been incubated for 6 days in vitro (6 DIV). Cells were fixed with 100% methanol at –20°C for 6 minutes and rinsed three times with 0.01 M PBS (pH 7.4). NGS (5%) was applied for 1 hour to block nonspecific binding of primary antibody. Each of the primary and secondary antibodies was applied separately; tissues were rinsed three times with 0.01 M PBS after each antibody application. Cultures were covered with Dabco, coverslipped, and observed within 24 hours.

Antibodies

Anti-GluR2/3 antibody—Polyclonal anti-GluR2/3 antibody raised against the amino acid sequence EGYNVYGIESVKI (850–862; Chemicon, Temecula, CA; AB1506; 1:100 dilution; Table 1) specifically labels GluR2 and GluR3 subunits, but not GluR1 and GluR4. Evaluations of anti-GluR2/3 antibody have been carried out using Western blot analysis of rat brain, showing that GluR2/3 antiserum was selective to GluR2 and GluR3 monomers (M_r = 108,000 kDa) but not to GluR1 nor GluR4 (Wenthold et al., 1992). Furthermore, immunocytochemistry studies tested antibody specificity on cell lines transfected with each of the four AMPAR cDNAs. These studies showed that anti-GluR2/3 antibody selectively recognized GluR2 and GluR3 subunits, but not GluR1, GluR4, GFP, or secondary antibody alone (Wenthold et al., 1992; Flores-Otero et al., 2007).

Anti-synaptophysin antibody—The monoclonal anti-synaptophysin antibody clone SVP-38 (Sigma-Aldrich, St. Louis, MO; S5768; 1:50 dilution; Table 1) recognizes a 38-kDa molecular weight band in Western blot analysis of coated vesicles, bovine chromaffin granules, and presynaptic vesicles from bovine brain (Wiedenmann and Franke, 1985; Gaardsvoll et al., 1988). Recent studies have confirmed this result; in fact, Western blot analysis of monoclonal anti-synaptophysin antibody showed a single band at the appropriate 38-kDa molecular weight (Wheeler et al., 2002; Morris et al., 2005), whereas immunocytochemical evaluation of transfected N2a cells showed that anti-synaptophysin

antibody selectively recognized synaptophysin-GFP but not SNAP-25-GFP, GFP, or secondary antibody alone (Flores-Otero et al., 2007).

Anti-BDNF antibody—Anti-BDNF antibody labeling was performed with two different polyclonal antibodies: one from Santa Cruz Biotechnology (Santa Cruz, CA; made against amino acids 128–147 of the human protein N-20; sc-546; 1:100 dilution) and the other from Abcam (Cambridge, MA; made against the full-length human protein; ab6201; 1:200 dilution; see Table 1). Of the two antibodies, the most extensive characterization has been reported for that generated by Santa Cruz Biotechnology. Western blot analysis has shown that Santa Cruz Biotechnology anti-BDNF antibody specifically recognized bands that corresponded to the pro-form and mature form of BDNF (~34 kDa and 13 kDa, respectively). Both bands were attenuated by preincubating anti-BDNF antibody with the appropriate peptide antigen and were unaffected by preincubating the antibody with NT-3 peptide antigen (Schimmang et al., 2003; Tan and Shepherd, 2006). Moreover, labeling of cerebellar granule neurons, used as a positive control, was eliminated upon preincubation of the BDNF antiserum with the corresponding antigenic peptide. Dot blot analysis also showed that the reactivity of this BDNF antiserum is abolished after blotting human recombinant BDNF onto membranes that were exposed to preabsorbed BDNF antiserum compared with those exposed to BDNF antiserum, both at 1:1,000 (Seki et al., 2003).

Anti-NT-3 antibody—The anti-NT-3 antiserum (made against the 11-amino-acid peptide YAEHKSHRGEY; Millipore, Bedford, MA; AB1527; lot PSO1410579; 1:100 dilution; Table 1) has been shown to recognize a 30-kDa band in Western blot analysis when tissues from different brain regions were used as a positive control (olfactory bulb, cortex, hippocampus, and cerebellum); however, this band was not detected in these samples when the recombinant of NT-3 was applied in excess amounts (Krause et al., 2008).

Anti-class IIIβ-tubulin antibody—To distinguish spiral ganglion neurons from surrounding satellite cells in the neuronal cultures, either a polyclonal or a monoclonal class IIIβ-tubulin neuron-specific antibody was applied (TUJ1; Covance, Berkeley, CA; PRB-435P; 1:200 dilution; and MMS-435P; 1:200 dilution; respectively). The class IIIβ-tubulin neuronal antibody recognized a 50-kDa band in Western blot analysis of rat brain (1:5,000) and MDCK lysate (1:500; Covance; PRB-435P and MMS-407R data sheet, respectively). Previous studies from this laboratory have utilized anti-β-tubulin labeling to demarcate neurons from background satellite cells at appropriate concentrations (Reid et al., 2004).

Anti-peripherin antibody—Polyclonal or monoclonal anti-peripherin antibody (Chemicon; AB-1530 and MAB-1527, respectively) was used to distinguish type II neurons from type I neurons in the apex and base tissue cultures (Mou et al., 1998; Hafidi, 1998). These antisera made against the N-terminus of rat peripherin recognized a 57-kDa band on Western blot analysis of intermediate filament-enriched cytoskeletal preparations, which was consistent with immunoflurescence experiments that showed specific labeling of filamentous cytoskeletal structures in cultured PC12 cells (Parysek et al., 1988).

To establish the appropriate anti-peripherin antibody concentration that labels exclusively type II spiral ganglion neurons, we used two different preparations. The first consisted of acute whole-mount preparations that were processed for immunolabeling immediately after dissection. This preparation, which essentially retains all neuronal processes, both afferent and efferent, allowed us to determine the appropriate concentrations in which anti-peripherin antibody did not label type I neurons. This was evaluated by determining that all fibers that terminated on the inner hair cells were unlabeled with peripherin, whereas some of the fibers projecting to the outer hairs cells were labeled (efferent fibers remained unlabeled with

peripherin antisera). The second preparation consisted of an organ of Corti culture that was incubated for 3 days in vitro in order to eliminate efferent processes. Because all of the processes innervating the outer hair cells consisted solely of type II neurons, we used these cultures to determine unequivocally that at appropriate concentrations all type II neurons were labeled with the anti-peripherin antibody. In these preparations 10.6% ± 3.1% (n = 4) of the neuronal soma were peripherin positive, which is consistent with the relative proportions of the type I/type II peripheral afferents in the ganglion.

Secondary antibodies—Secondary antibodies included Alexa fluor 488-conjugated anti-mouse (Invitrogen, Carlsbad, CA; 11017), Alexa fluor 488-conjugated anti-rabbit secondary antibodies (Invitrogen; 11008), Alexa fluor 488-conjugated anti-sheep secondary antibodies (Invitrogen; 11015), Alexa fluor 594-conjugated anti-rabbit (Invitrogen; 11012), Alexa fluor 594-conjugated anti-mouse (Invitrogen; 11005), Alexa fluor 350-conjugated anti-mouse (Invitrogen; 11068), and Alexa fluor 350-conjugated anti-rabbit (Invitrogen; 11069).

Image acquisition and quantitative analysis

Fluorescence-labeled images of cochlear sections and isolated spiral ganglion neuronal preparations were acquired with a Hamamatsu 1394 Orca-ER camera using IPLab Scientific Imaging Software (BD Biosciences, Franklin Lakes, NJ) saved in Tiff format and analyzed with Adobe Photoshop v7.0 (Adobe Systems, San Jose, CA). The number of cochlear turns varied between paraffin-embedded postnatal and adult cochlea sections such that no section contained both the extreme apical and the extreme basal regions. Therefore, to compare the distribution patterns of anti-GluR2/3 and anti-synaptophysin antibodies along the cochlea length, we referred to neuronal groups as apical or basal according to their relative locations. In all cases, multiple sections from the same animal were utilized in order to confirm intraexperimental reliability, and sections from more than one animal were utilized in order to establish interexperimental consistency; in total, three or more sections were analyzed for statistical comparisons.

Measurements of antibody irradiance were made from nonadjusted images after image acquisition with identical exposure times; for the purposes of illustration, images were adjusted equally such that irradiance intensity can be compared between conditions for each experiment. Images in Figures 5b,c and 6b,c were optimized with 2-D blind deconvolution algorithyms (IPLab) with the following parameters: PSF iterations = 2; super res factor = 1, guard band (pixels) = 5. Antibody concentrations, exposure times, and photographic adjustments were selected to avoid saturation, which would make it impossible to detect staining differences along the cochlear frequency contour. Antibody irradiance levels were measured according to the methodology described by Flores-Otero et al. (2007). In brief, measurements from each neuronal soma were adjusted for background levels by subtracting the average of four measurements taken from the surrounding region. For hair cell measurements, the entire soma area in a single section was averaged (dotted lines, Figs. 5b,c, 6b,c), excluding the nuclear area from which the background measurements were subtracted. By evaluating average antibody irradiance on a cell-by-cell basis, we ensure that our analysis is independent of any changes in cell size or soma packing density. Nevertheless, it should be noted that, despite the care in making accurate antibody irradiance measurements, the values that we report are not directly related to protein levels; instead, they reflect relative differences or similarities in antibody labeling between regions or cells. As reported previously, we evaluated staining levels in the neuronal somata to use a single cellular location that possessed high protein levels, rather than having to evaluate the typically low levels in differential subcellular regions. This approach was particularly critical for spiral ganglion neurons in vitro, because antibody labeling, although observed at terminal endings, was too sparse and widely distributed for accurate, repeatable

measurements above background. In this study, we focused on evaluating protein levels, rather than determining the precise functional consequences; others, however, have demonstrated that AMPA receptor levels in spiral ganglion neuronal somata closely reflect auditory function (Chen et al., 2007). Statistical comparisons were made using Student's two-tailed paired *t*-test. SEM is indicated by error bars.

RESULTS

Type I/type II staining patterns

Previous evaluations of synaptic protein distributions had focused on the overall population of neurons derived from discrete apical and basal regions of the cochlea. Because type II neurons make up such a small percentage of the neuronal population, our conclusions based on overall averages largely reflected type I neuronal characteristics. However, because type I and type II spiral ganglion afferents have very different functions as evidenced by their distinctive peripheral and central synaptic inner-vation patterns, we extended our earlier studies by specifically comparing the two neuronal types. As reported in previous studies from this and other laboratories, the neurofilament peripherin is present in both classes of neuron but is highly enriched in the type II neurons (Mou et al., 1998; Hafidi, 1998; Reid et al., 2004). By using appropriate concentrations of anti-peripherin antibody, established with organ of Corti preparations (see Matetrials and Methods), we were able to identify putative type II spiral ganglion neurons in vitro. Examples of differential labeling with anti-peripherin antibody are shown in Figure 1. Two clusters of basal neurons from different regions of the same culture dish showed some strongly labeled cells, whereas others in close association were essentially unstained (Fig. 1a–d).

We examined whether the tonotopic differences in anti-AMPAR antibody labeling were present in type II neurons and whether potential differences would be impacted by the requirement for convergent innervation. As shown in Figure 1a,d, the relatively high levels that would be expected in basal neurons were relatively uniform for all neurons shown, regardless of whether they were labeled with anti-peripherin antibody (Fig. 1b,c). Quantitative analysis of anti-GluR2/3 irradiance levels for a single experiment designed to compare the relative amounts of AMPAR protein for both apical and basal type I and II spiral ganglion neurons is shown in Figure 1e–g. It should be noted that this particular culture contained an unusually large number of type II compared with type I neurons. Nevertheless, we chose this example for illustration because it enabled us to make comparisons between the two classes of cells within a single experiment. The histograms that resulted from the analysis did not show an obvious distinction between type I and type II spiral ganglion neurons either from the apex (Fig. 1e) or from the base (Fig. 1f). Superimposed normalized Gaussian fits (Fig. 1g) show, however, a clear apical/basal difference in anti-GluR2/3 antibody labeling for both type I and type II neurons, with apical type I and type II neurons both displaying relatively low levels of anti-GluR2/3 compared with their basal counterparts.

We found in this study and previous studies (Mou et al., 1998; Reid et al., 2004) that our in vitro preparations generally contained a low percentage of type II neurons, as expected from the relative paucity of these cells in vivo. It is for this reason that measurements from this category of neuron are necessarily low in number for each individual experiment. Therefore, we evaluated the distribution of anti-GluR2/3 antibody irradiance from this small population of cells by combining all of our measurements from six separate experiments. As shown in Figure 1h–j, the combined analysis replicated the findings from the single experiment. Histograms and Gaussian fits of apical type I anti-GluR2/3 antibody irradiance measurements have a mean value very similar to that of the apical type II neurons (Fig. 1h). The mean anti-GluR2/3 antibody irradiance level of the basal type I neurons derived from

Gaussian fits to combined data also overlapped with those from the basal type II neurons (Fig. 1i). By normalizing the Gaussian fits and plotting them on the same graph, it is clear that measurements from both classes of apical spiral ganglion neuron are consistent with their possessing lower AMPAR protein levels compared with the two classes of basal neurons (Fig. 1j).

The observations described above were also borne out when the mean values were averaged from each separate experiment. Anti-GluR2/3 antibody irradiance was higher in basal neurons than in apical neurons and was distributed equally between type I and type II neurons (Fig. 2). The apex/base difference was statistically significant at the $P < 0.01$ level when evaluated from six experiments. Apical type I spiral ganglion neurons had an average irradiance of 9.9 ± 0.7, which was essentially indistinguishable from that observed in apical type II neurons (9.8 ± 0.7). These values differed significantly from the basal type I (15.7 ± 1.0) and type II (15.8 ± 0.8) measurements, respectively. Thus, the two classes of spiral ganglion neuron do not appear to differ in their AMPAR content within each tonotopic location, but both vary along the cochlear partition.

In addition to their separate peripheral innervation patterns, type I and type II spiral ganglion neurons also synapse onto distinct classes of neurons centrally (Brown et al., 1988). Our previous work showed that spiral ganglion neurons display apex/base differences in levels of the presynaptic protein synaptophysin, with the added complexity that synaptophysin staining patterns are heterogeneous within apical neurons (Flores-Otero et al., 2007). Therefore, we sought to establish or rule out whether the heterogeneity could be attributed to a difference between type I and type II neurons. To examine this issue fully, we initially compared the anti-synaptophysin antibody staining patterns of type I and type II spiral ganglion neurons derived from the apex of the cochlea. As shown in Figure 3, heterogeneous labeling was found within neurons classified as type I (Fig. 3a–d) and type II (Fig. 3e–h) based on their anti-peripherin staining intensity. Neurons without appreciable anti-peripherin antibody staining (Fig. 3c) showed clear anti-synaptophysin antibody labeling heterogeneity (Fig. 3a,d), as did those with robust anti-peripherin antibody labeling (Fig. 3e–h). An example of measurements taken from a population of apical neurons within a single experiment showed that apical type I and type II neurons showed a wide range of irradiance levels. In the case of the type I spiral ganglion measurements, the histograms could be fitted with a double Gaussian function. Measurements of the type II neurons showed a single function but with an exceptionally large variance (Fig. 3i). In contrast to this, measurements from both type I and type II basal neurons from the same experiment showed that both classes of neuron had smaller overall irradiance levels and ranges, which were virtually overlapping (Fig. 3j).

Because type II neurons were fairly rare in each experiment, we combined six separate experiments to increase our number of observations. This approach confirmed and refined the findings from a single experiment by permitting more accurate Gaussian fits to be made to the larger data sets. Apical type I and type II measurements were both well fitted with double Gaussians having similar means for each distribution (20.5 and 45.4 compared with 25.0 and 56.5 for type I and II neurons, respectively; Fig. 3l). Basal neurons, on the other hand, showed tighter distributions that essentially overlapped for type I (12.7) and type II (11.0) neurons (Fig. 3m). By normalizing the Gaussian fits and overlapping them on the same graph, it was clear that the means of the double Gaussian functions that best describe anti-synaptophysin irradiance levels in both classes of apical neurons were consistently higher than the single Gaussians that best describe anti-synaptophysin antibody irradiance levels in basal neurons (Fig. 3n).

Observations from the individual measurements were also reiterated when the mean values from each separate experiment were averaged. The higher staining intensity in apical neurons made the similarity between type I and type II neurons more obvious, but, even with the lower anti-synaptophysin irradiance levels in basal cells, the equal distribution between classes of neurons was clear (Fig. 4). Apical type I spiral ganglion neurons had an average irradiance level of 27.2 ± 3.5, very close to that observed in apical type II neurons (28.3 ± 3.9). These values, however, differed significantly from the basal type I (13.8 ± 0.6) and type II (14.0 ± 0.8) measurements. The two classes of spiral ganglion neuron, therefore, do not appear to differ in their presynaptic protein levels within each frequency location but differ similarly along the tonotopic map.

Neurotrophin distribution in the organ of Corti

It thus appears that for both the presynaptic synaptophysin and the postsynaptic GluR2/3, it is the region from which the neurons are located that appears to dictate their protein levels rather than the specific type of neuron. To test this prediction, we examined the distribution of two neurotrophins, BDNF and NT-3, that have been shown to exert powerful regulatory effects on pre-synaptic and postsynaptic proteins as well as on specific voltage-gated ion channels (Adamson et al., 2002a; Flores-Otero et al., 2007). Because the hair cell receptors possess these trophic molecules (Fritzsch et al., 2004; Flores-Otero et al., 2007; Sugawara et al., 2007), we decided to evaluate the distribution of well-characterized anti-BDNF and anti-NT-3 antibodies in the inner and outer hair cells within different regions of the cochlear partition. Furthermore, because type I neurons exclusively innervate inner hair cells and type II neurons exclusively innervate outer hair cells at this age (Echteler, 1992), we were curious to see whether the localization of BDNF and NT 3 within these receptor cells could be predicted by our observations of the protein levels that they purportedly control in the two classes of postnatal spiral ganglion neurons. We hypothesized that BDNF, the neurotrophin responsible for up-regulating GluR2/3 in basal neurons, would be graded from base to apex and would be distributed relatively equally between inner and outer hair cells. As shown in Figure 5, both of these conditions appear to exist. We noted a subtle, yet significant, increase in anti-BDNF irradiance levels in more basally located receptor cells compared with more apically located ones in the same postnatal sections. Moreover, inner and outer hair cells appeared to be relatively uniformly labeled. The areas of comparison for one such example are shown in the merged, low-magnification view of a midmodiolar section in Figure 5a (dotted boxes). Side-by-side comparison of the high-magnification images of two such regions exemplifies the enriched anti-BDNF antibody labeling of basal inner and outer hair cells (Fig. 5c, inner hair cells surrounded by dashed line; outer hair cells surrounded by dotted line) compared with the apical ones (Fig. 5b, inner hair cells surrounded by dashed line; outer hair cells surrounded by dotted line). Quantitative analysis of multiple measurements (15 apical; 20 basal) from 10 sections of three different preparations, using two different anti-BDNF antibodies shows that these differences are significant at the $P < 0.01$ level (Fig. 5d). Apical inner and outer hairs cells with average anti-BDNF irradiance levels of 10.7 ± 0.6 and 11.7 ± 0.6, respectively, differed significantly from inner and outer hair cells in the base (16.55 ± 0.8, and 16.6 ± 1.0 respectively). No systematic differences were noted between rows of outer hair cells. When the labeling for the two different antibodies was evaluated separately, we found that each produced the same basic results. Therefore, with two different anti-BDNF antibodies, either in combination or separately, we observed a pattern of protein distribution (Fig. 5d) that compared remarkably well with the levels of GluR2/3 (Fig. 2).

Because NT-3 has effects opposite to those exerted by BDNF, we hypothesized that this neurotrophin would be enriched in the apex but be distributed relatively equally between inner and outer hair cells. As shown in Figure 6, both of these conditions were satisfied.

There was a significant increase in anti-NT-3 irradiance levels in more apically located receptor cells compared with more basally located ones in the same postnatal sections. In addition, inner and outer hair cells appeared to be relatively uniformly labeled. The areas of comparison for one such example are shown in the merged, low-magnification view of a midmodiolar section in Figure 6a (dotted boxes). Side-by-side comparison of the high-magnification images of two such regions illustrates a discernible enrichment of anti-NT-3 antibody labeling in apical inner and outer hair cells (Fig. 6c, inner hair cells surrounded by dashed line; outer hair cells surrounded by dotted line) compared with the basal ones (Fig. 6b, inner hair cells surrounded by dashed line; outer hair cells surrounded by dotted line). Quantitative analysis of multiple measurements (7 apical, 10 basal) from five sections of two different preparations shows that these differences are significant at the $P < 0.01$ level (Fig. 6d). Apical inner and outer hair cells with an average anti-NT-3 irradiance level of 18.3 ± 0.8 (n = 7) and 19.7 ± 1.1 (n = 7), respectively, differ significantly from inner and outer hair cells in the base (11.4 ± 0.4, n = 10; and 12.0 ± 0.6, n = 10, respectively). No systematic differences were noted between rows of outer hair cells. These results were, again, consistent with our expectations and furthermore demonstrated a pattern of protein distribution (Fig. 6d) that compared remarkably well with the levels of synaptophysin (Fig. 4).

Gradations of synaptic proteins in the spiral ganglion: postnatal sections

From evaluating the synaptic protein distribution within type I and type II neurons, it is evident that levels of GluR2/3 and synaptophysin do not differ between cell type but rather vary as a function of cochlear location. To determine whether this apex/base difference represents a strictly graded relationship, we extended our analysis from the extreme regions of the apex and base to midregions of the cochlea. By examining this issue in animals of the same age used previously for electrophysiological analysis (Liu and Davis, 2007), we could determine how synaptic protein distributions compare with timing- vs. threshold-related features.

For this approach, we carried out an immunocytochemical analysis of cochlear sections from postnatal animals that contained three or more separate regions of spiral ganglion neurons, thus allowing us to determine how protein content varied from one end of the cochlea to the other. This is an exacting approach because multiple regions of the spiral ganglion can be evaluated within a single section, removing any doubt that changes could have occurred in staining or photographic acquisition procedures between neuronal regions.

From these studies, we determined that the intensity of anti-GluR2/3 antibody irradiance progressively increased from apical to basal regions. A low-magnification merged image of anti-GluR2/3 and anti-β-tubulin antibody staining indicates four separate regions that were evaluated within the spiral ganglion (Fig. 7a). Regions that had a more apical location (Fig. 7b,c) showed reduced irradiance compared with those with a more basal location (Fig. 7d,e). All regions had similar levels of anti-β-tubulin antibody labeling indicating that antibody penetration and section thickness did not account for the observed differences (Fig. 7f–i). A higher magnification of these regions (dotted boxes) shows that the apicalmost area (Fig. 7j) has substantially lower anti-GluR2/3 antibody irradiance compared with the most basal region (Fig. 7m) and that the areas in between (Fig. 7k,l) show an orderly progression that is suggestive of a systematic gradient along the tonotopic axis. To determine whether this was a consistent finding, five separately processed sections of neurons located in four different regions of the spiral ganglion, taken from two different animals, were evaluated. The average of these measurements substantiated what we observed in a single section, that antibody irradiance increased in a smooth progression from apical to basal cochlear regions. The average irradiances of the apical, midapical, midbasal, and basal regions were 24.5 ± 2.5, 29.7 ± 4.2, 39.8 ± 5.4, and 50.1 ± 4.1, respectively. Each condition differed significantly

from the others, as indicated in Figure 7n ($P < 0.01$), except for the specific comparison between apical and midapical regions, which was close to the 0.05 level ($P = 0.052$). By comparison, anti-β-tubulin antibody irradiance levels averaged for the same five experiments had similar values for apical, midapical, midbasal, and basal regions (17.6 ± 2.5, 18.2 ± 2.7, 18.5 ± 2.6, and 18.5 ± 2.8, respectively), indicating that the tonotopic variation was specific for AMPA receptors.

Anti-synaptophysin antibody labeling was also examined in postnatal sections from animals of the same age in order to determine the distribution pattern of this pre-synaptic protein. The expected enrichment in apical regions, opposite to that of the AMPA receptors, was readily observed. As shown in Figure 8, not only was anti-synaptophysin antibody labeling enriched in apical regions, but graded irradiance levels were noted in three separate ganglionic areas (Fig. 8b–d). Anti-β-tubulin antibody irradiance levels, however, did not differ between these regions (Fig. 8e–g). We chose areas of similar neuronal density to evaluate at high magnification (Fig. 8b–g, dotted squares). In each instance, the apical neurons (Fig. 8h) displayed the highest irradiance, the basal regions displayed the lowest irradiance (Fig. 8j), and the midregion irradiance levels spanned the difference (Fig. 8i). To determine whether this was a consistent finding, seven separately processed sections of neurons located in three different regions of the spiral ganglion, taken from three different animals, were evaluated. The average of these measurements again reiterated our observations within a single section (Fig. 8k). Apical regions had the highest irradiance levels (22.4 ± 2.5), midregions were intermediate (16.2 ± 2.6), and basal regions were the lowest (13.1 ± 1.9), indicating that a gradient appears to extend from the apex to the base. When compared statistically, the differences between all of these conditions was significant at levels indicated in Figure 8k. By comparison anti-β-tubulin antibody irradiance levels averaged for the same seven experiments had similar values for apical, middle, and basal regions (19.5 ± 1.8, 19.4 ± 1.8, and 19.4 ± 1.7, respectively), indicating that the tonotopic variation was specific for synaptophysin.

During the course of this study, we noted that, within any particular cochlear region, anti-GluR2/3 antibody labeling was uniform, whereas anti-synaptophysin labeling was relatively heterogeneous. Detailed evaluation of anti-synaptophysin antibody staining revealed that differences between neighboring neurons had a patterned distribution in postnatal sections. When we analyzed eight stained tissue sections, we noted that seven of them had one or more regions of neurons that displayed local gradients. The example shown in Figure 9 exemplifies the progression of anti-synaptophysin labeling that was lowest in neurons situated close to the scala vestibuli (SV) and increased progressively in neurons situated closer to the scala tympani (ST), orthogonal to the tonotopic gradient (Fig. 9b). For synaptophysin, therefore, our analysis revealed two superimposed gradients, one that showed the highest irradiance levels in the apex compared with the base (solid arrow, Fig. 9b) and another with the highest irradiance in neurons closer to the scala tympani compared with the scala vestibuli (dotted arrow, Fig. 9b). Irradiance levels quantified for each of the three regions highlighted in Figure 9b showed that the local gradient from ST to SV was retained, but with progressively lower irradiance in neurons at more basal locations (Fig. 9d–f). Quantitative analysis of three separate preparations in which quantitative measurements could be obtained in three distinct frequency regions revealed that anti-synaptophysin irradiance levels progressively declined from SV to ST, while still retaining a tonotopic gradient (Fig. 9g–i). Average irradiance levels from neurons in apical, low-frequency regions were lowest for those closest to the SV (22.8 ± 2.5) compared with those in regions progressively closer to the ST (31.7 ± 3.5 and 49.0 ± 3.0, respectively). This was true for each of three groups of neurons located progressively from SV to ST in midfrequency regions (17.0 ± 1.9, 25.2 ± 2.2, and 35.9 ± 2.6, respectively) and higher frequency regions (14.4 ± 1.3, 21.2 ± 2.1, and 28.7 ± 2.5, respectively). Therefore, our

analysis of cochlear sections revealed that the differential anti-synaptophysin labeling observed in vitro not only is present in vivo but is patterned systematically along the SV-ST contour.

Gradations of synaptic proteins in the spiral ganglion: adult sections

To determine whether the protein distributions described above contribute to, or result from, developmental or functional aspects of signaling, we evaluated sections obtained from adult animals. AMPAR distribution was evaluated with the same GluR2/3 antibody utilizing an HRP staining protocol (see Materials and Methods). Regions selected for detailed examination (highlighted in Fig. 10a, dotted squares) are shown at a higher magnification in Figure 10b,c. Side-by-side comparison of these areas shows a stark regional difference, with basal neurons having higher density levels than apical ones, consistent with our previous postnatal in vivo and in vitro findings. This observation was similar for all sections examined. As shown in Figure 10d, basal regions (25.2 ± 6.5) had a significantly higher density ($P < 0.05$) than apical regions (14.6 ± 4.5) measured for four different preparations. Additionally, we evaluated laterally cut modiolar sections, which included an elongated region of neurons that spanned the cochlear contour (Fig. 11). This view of the ganglion provided further evidence of a detectable and systematic gradient along the apical–basal axis. Although the region is relatively short, side-by-side comparisons do show that the more basal neurons (Fig. 11d) are stained slightly darker than those at progressively more apical regions (Fig. 11b,c). Quantitative measurements (Fig. 11a) confirmed the visual impression, showing that the protein distribution for GluR2/3 is graded along the tonotopic axis in the adult cochlea.

Synaptophysin distribution was also evaluated in adult sections utilizing the HRP staining protocol. Regions of the ganglion having similar neuronal density (Fig. 12a, dotted squares) are shown at a higher magnification in Figure 12b,c. Side-by-side comparison of these areas shows an obvious regional difference consistent with our postnatal in vivo and in vitro findings, such that the apical regions have higher HRP density than the basal ones. This observation was consistent in all of the sections that we examined. As shown in Figure 12d, apical regions have a significantly higher density level (25.5 ± 4.1; $P < 0.05$) than basal ones (13.3 ± 2.4) for six separate experiments from three different preparations. Again, laterally cut modiolar sections were utilized so that numbers of neurons could be evaluated along the contour of the cochlea. These revealed a detectable gradient along the basal–apical axis. Side-by-side comparisons of the regions farthest from one another (Fig. 13b,d, dotted squares) showed that the more apical region was stained slightly darker than its neighboring, more basal end. Measurements from the specific basal section highlighted in Figure 13a showed that the highest antibody enrichment changed progressively along this section of neurons (Fig. 13a, inset). These results, therefore, are consistent with the idea that the differential presynaptic and postsynaptic protein distributions characterized in postnatal neurons are also present in the adult, fully developed spiral ganglion and that they contribute to auditory function in the mature inner ear.

DISCUSSION

By examining somatic presynaptic and postsynaptic protein content in neurons of the spiral ganglion, we have gained new insights into the functional organization of the auditory primary afferents. We focused our attention on three aspects: differences between the type I and the type II neurons, longitudinal and local distribution patterns along the tonotopic axis, and tissue obtained from postnatal and adult animals. Each comparison was made for a specific reason. First, type I and type II neurons show dramatic differences in their structure and ganglionic organization and identifying similarities or differences between them could help in understanding their functional significance. Second, the comparison between

neighboring neurons allows one to quantify the constancy of tonotopic gradients and the potential for parallel processing of parameters such as sound intensity within a limited frequency region. Third, by using sections from different-aged animals, we can determine whether gradients identified in developing animals persist into adulthood and would therefore be likely to be significant contributors to function in the mature inner ear. The data that we obtained provide further support for the idea that spiral ganglion neurons possess electrophysiological specializations along the tonotopic axis that are smoothly graded and are present in both immature and adult animals.

Type I vs. type II neurons

As discussed below, although we identified apex/base differences in the spiral ganglion neurons, our initial comparison between the two classes of primary afferent did not reveal differences between type I and type II neurons for either the postsynaptic anti-GluR2/3 antibody or the presynaptic anti-synaptophysin antibody. A straightforward conclusion, therefore, is that, although the synaptic properties of apical type I and type II neurons can differ from their basal counterparts, they are not different from each other. The surprising similarity in staining levels, however, is open to alternative interpretations. One might have expected, for example, that the type II neurons with their propensity to make numerous synaptic connections with outer hair cell receptors would have exhibited AMPAR enrichment compared with type I neurons that make a single synaptic connection with only one inner hair cell. The central trajectory of the type I and type II spiral ganglion neurons is also distinctive. While both classes of afferent innervate multiple regions within the cochlear nucleus of the brainstem, they project to different cell types with diverse presynaptic specializations (Brown et al., 1988; Berglund et al., 1996; Benson and Brown, 2004). One of these specializations, the endbulb of Held, is a calyx-type ending that is elaborated exclusively by type I spiral ganglion neurons, which project onto bushy cells of the AVCN (Oertel, 1999; Trussell, 2002; Carr, 2004). One might speculate that these large synaptic specializations require enhanced presynaptic proteins to carry out their function, suggesting an enhancement of synaptophysin in type I compared with type II afferents. Moreover, intrinsic electrophysiological parameters must also be considered. Whole-cell recordings from identified type I and type II spiral ganglion neurons in vitro showed that, compared with their type I counterparts, type II neurons displayed slower accommodation and kinetics with lower thresholds and higher input resistances (Reid et al., 2004). Thus additional differences may be present that were not identified here. Despite their utility in these and other studies, the anti-GluR2/3 and anti-synaptophysin antibodies are not indicators of the distinctive synaptic features of type I and type II neurons. In addition, processes that scale synaptic strength may be at work, reducing, for example, the density of synaptic AMPARs in type II neurons to compensate for the lower thresholds displayed by these cells. Although the small number of type II neurons in single tissue sections precludes a detailed analysis in preparations, future in vitro work will include assessment of other pre- and post-synaptic components to address this question in greater depth.

The similarity of type I and type II neurons in a given cochlear region led to a prediction about neurotrophin content, which we evaluated by quantifying anti-neurotrophin antibody immunofluorescence within the inner and outer hair cells that form selective synapses on type I and type II afferents, respectively. Because the neurotrophins BDNF and NT-3 regulate synaptic protein composition within the spiral ganglion (Flores-Otero et al., 2007), as a first estimate one might expect that these neurotrophin levels vary regionally between high- and low-frequency areas yet remain equivalent in inner and outer hair cells. This hypothesis is based on earlier work in which we showed that BDNF up-regulates specific ion channel subunits ($K_v1.1$, $K_v3.1$, K_{Ca}) and postsynaptic proteins localized preferentially in basal neurons, whereas NT-3 up-regulates ion channel subunits ($K_v4.2$) and presynaptic

proteins localized preferentially in apical neurons (Adamson et al., 2002a; Flores-Otero et al., 2007). Therefore, the expectation is that BDNF and NT-3 would be found in higher amounts in the basal and apical hair cells, respectively. This presumed localization was supported by our results obtained with a functional bioassay using cocultures of hair cell microisolates with spiral ganglion neuron explants. Presynaptic and postsynaptic antibody labeling of spiral ganglion neurons was altered predictably when cocultured with hair cell microisolates from apical and basal regions of the organ of Corti; moreover, the effects were blocked by the appropriate function-blocking anti-neurotrophin antibody (Flores-Otero et al., 2007). This approach provided direct evidence that neurotrophins secreted from the specialized cells within the organ of Corti release the appropriate amount and type of neurotrophin to account for the distinct levels of synaptic protein that we observed in apical and basal spiral ganglion neurons. The immunolocalization of BDNF and NT-3 presented herein, for which we found that the inner and outer hair cells within each region have similar neurotrophin levels, further strengthen this model and are consistent with studies evaluating NT-3 promoter activity in the organ of Corti (Sugawara et al., 2007) and our previous bioassay analysis. It is important to emphasize, however, that the relationship between intracellular neurotrophin protein levels and the effects on their cellular targets is not simple. The density and types of high affinity receptors that each class of neuron possesses (Reichardt, 2006) along with the mechanism of neurotrophin release (Canossa et al., 1997; Farhadi et al., 2000; Hempstead, 2006) are examples of additional factors that could contribute to the overall regulatory control. In fact, observations that surface AMPA receptors are dynamically regulated and correlate with auditory sensitivity demonstrate the complexity of the synaptic interactions between hair cell receptors and spiral ganglion neurons (Chen et al., 2007). It is possible that our observations represent tonotopic set points that are regulated dynamically by neuronal activity.

Does local heterogeneity represent a level of parallel processing?

The initial events that lead to sensory perception classically involve parallel processing. In the auditory system, evidence for this can be found at many levels, starting with type I neurons innervating single hair cells that possess different threshold levels and spontaneous rates (Liberman, 1982). Neurons most responsive to low-intensity sounds are localized to the hair cell membrane closest to the nerve entry, whereas neurons with elevated threshold levels receive synapses from the opposite side of the hair cell. Thus, each individual hair cell has the potential to comprise a “hypercolumn” that provides input to a set of type I afferents each with the same characteristic frequency but activated by different sound intensities. It would not be surprising, therefore, if the endogenous specializations of neurons within a single frequency region are tailored to carry out the processing and transmission requirements that underlie this and other aspects of neural coding.

We examined the heterogeneity of staining intensity in restricted tonotopic regions to evaluate whether cell-to-cell differences could be assigned to differences between or within afferent classes. By taking this approach, we observed that AMPAR labeling was relatively homogeneous in postnatal neurons, whether evaluated in tissue sections or in vitro. By contrast, anti-synaptophysin antibody labeling was consistently heterogeneous both in vitro and in apical regions of postnatal tissue sections. We also noted that cells were labeled with different anti-synaptophysin antibody intensities in adult sections, although this should be viewed as preliminary because we were restricted to HRP staining protocols that precluded colabeling with anti-β-tubulin antibody in a single section. Nevertheless, these observations were consistent with our previous work showing that the heterogeneity of anti-synaptophysin antibody staining was greater in apical neurons and in neurons that had been exposed to NT-3. This finding prompted us to determine whether these observations were due to differences within or between neuronal classes. Because these types of experiments

require numerous measurements in order to construct histograms that can be well fitted with Gaussian functions, we confined our analysis to neurons in vitro because of the large number of apical and basal neurons that could be assessed for each experiment.

By distinguishing type I from type II neurons with anti-peripherin antibody, we found that synaptophysin heterogeneity was clearly present in both putative type I and type II spiral ganglion neurons. It should be noted that this presynaptic protein is one of many that have been reported to have different staining patterns within a specific tonotopic location of the spiral ganglion (Romand et al., 1990; Lopez et al., 1995, 2003; Rosenblatt et al., 1997; Flores-Otero et al., 2007). Much like what has been postulated for retinal ganglion cells (Wassle, 2004), it is possible that these proteins either contribute to or result from specific aspects of parallel processing. Furthermore, the relationship of synaptophysin gradients orthogonal to the tonotopic axis could draw parallels to the ganglionic organization of spontaneous rate within the modiolus of cat (Leake et al., 1992).

Gradients across the tonotopic map in postnatal and adult animals

A final issue that we explored by examining the distribution patterns of synaptic proteins in the spiral ganglion is their relationship to the tonotopic map. Because the primary cochlear organization is one of systematically graded specializations to enhance frequency detection, the presence of a gradient that corresponds to frequency can be a powerful indicator of the relevance of any specific feature. Our previous examination of the organization of presynaptic and postsynaptic proteins focused on the extreme ends of the cochlea, representing frequencies at opposite ends of the spectrum (Flores-Otero et al., 2007). Although highly informative, these studies did not allow us to determine unequivocally whether these proteins were graded or form other patterns, such as a step-like function or nonmonotonic functions. Based on our immunolabeling data from tissue sections, we noted that all of our observations were consistent with AMPARs forming a smooth gradient from base to apex and synaptophysin forming a smooth gradient in the opposite orientation, from apex to base.

Beyond the auditory and other sensory systems, graded distributions of molecules are commonly seen during development of patterned structures (Tabata, 2001; Patterson, 2001). In the auditory system, aside from the final mitosis that proceeds from the apex to the base (Ruben, 1967), most other features mature progressively from the base to the apex (Rubel, 1978). These stereotypic developmental patterns foretell the final organization of an end organ that ultimately displays gradients of cellular and mechanical properties that systematically vary from one end to the other (Fettiplace and Fuchs, 1999; Robles and Ruggero, 2001; Rubel and Fritzsch, 2002; Raphael and Altschuler, 2003). By comparing sections from postnatal and adult tissue, we show that graded amounts of pre- and postsynaptic proteins are seen in the mature cochlea. The findings reported herein add to our understanding of the neuronal organization of the auditory system by showing that these elegant patterns that begin with the hair cells extend beyond the cochlear partition to the primary afferents.

Supplementary Material

Refer to Web version on PubMed Central for supplementary material.

Acknowledgments

We thank Dr. Mark R. Plummer for discussions and critical reading of the manuscript. Expert technical support was provided by Yun Hsu and Hui Zhong Xue.

Grant sponsor: National Institutes of Health; Grant number: RO1 DC01856 (to R.L.D.); Grant sponsor: Gates Millennium Scholarship (to J.F.-O.).

LITERATURE CITED

Adamson CL, Reid MA, Davis RL. Opposite actions of brain-derived neurotrophic factor and neurotrophin-3 on firing features and ion channel composition of murine spiral ganglion neurons. J Neurosci. 2002a; 22:1385–1396. [PubMed: 11850465]

Adamson CL, Reid MA, Mo ZL, Bowne-English J, Davis RL. Firing features and potassium channel content of murine spiral ganglion neurons vary with cochlear location. J Comp Neurol. 2002b; 447:331–350. [PubMed: 11992520]

Benson TE, Brown MC. Postsynaptic targets of type II auditory nerve fibers in the cochlear nucleus. J Assoc Res Otolaryngol. 2004; 5:111–125. [PubMed: 15357415]

Berglund AM, Benson TE, Brown MC. Synapses from labeled type II axons in the mouse cochlear nucleus. Hear Res. 1996; 94:31–46. [PubMed: 8789809]

Brown MC, Berglund AM, Kiang NY, Ryugo DK. Central trajectories of type II spiral ganglion neurons. J Comp Neurol. 1988; 278:581–590. [PubMed: 3230171]

Canossa M, Griesbeck O, Berninger B, Campana G, Kolbeck R, Thoenen H. Neurotrophin release by neurotrophins: implications for activity-dependent neuronal plasticity. Proc Natl Acad Sci U S A. 1997; 94:13279–13286. [PubMed: 9371837]

Carr CE. Timing is everything: organization of timing circuits in auditory and electrical sensory systems. J Comp Neurol. 2004; 472:131–133. [PubMed: 15048681]

Chen Z, Kujawa SG, Sewell WF. Auditory sensitivity regulation via rapid changes in expression of surface AMPA receptors. Nat Neurosci. 2007; 10:1238–1240. [PubMed: 17828255]

Echteler SM. Developmental segregation in the afferent projections to mammalian auditory hair cells. Proc Natl Acad Sci U S A. 1992; 89:6324–6327. [PubMed: 1631126]

Farhadi HF, Mowla SJ, Petrecca K, Morris SJ, Seidah NG, Murphy RA. Neurotrophin-3 sorts to the constitutive secretory pathway of hippocampal neurons and is diverted to the regulated secretory pathway by coexpression with brain-derived neurotrophic factor. J Neurosci. 2000; 20:4059–4068. [PubMed: 10818141]

Fettiplace R, Fuchs PA. Mechanisms of hair cell tuning. Annu Rev Physiol. 1999; 61:809–834. [PubMed: 10099711]

Flores-Otero J, Xue HZ, Davis RL. Reciprocal regulation of presynaptic and postsynaptic proteins in bipolar spiral ganglion neurons by neurotrophins. J Neurosci. 2007; 27:14023–14034. [PubMed: 18094241]

Fritzsch B, Farinas I, Reichardt LF. Lack of neurotrophin 3 causes losses of both classes of spiral ganglion neurons in the cochlea in a region-specific fashion. J Neurosci. 1997; 17:6213–6225. [PubMed: 9236232]

Fritzsch B, Tessarollo L, Coppola E, Reichardt LF. Neurotrophins in the ear: their roles in sensory neuron survival and fiber guidance. Prog Brain Res. 2004; 146:265–278. [PubMed: 14699969]

Gaardsvoll H, Obendorf D, Winkler H, Bock E. Demonstration of immunochemical identity between the synaptic vesicle proteins synaptin and synaptophysin/p38. FEBS Lett. 1988; 242:117–120. [PubMed: 2462508]

Hafidi A. Peripherin-like immunoreactivity in type II spiral ganglion cell body and projections. Brain Res. 1998; 805:181–190. [PubMed: 9733963]

Hempstead BL. Dissecting the diverse actions of pro- and mature neurotrophins. Curr Alzheimer Res. 2006; 3:19–24. [PubMed: 16472198]

Krause S, Schindowski K, Zechel S, von Bohlen und Halbach O. Expression of trkB and trkC receptors and their ligands brain-derived neurotrophic factor and neurotrophin-3 in the murine amygdala. J Neurosci Res. 2008; 86:411–421. [PubMed: 17828769]

Leake PA, Snyder RL, Merzenich MM. Topographic organization of the cochlear spiral ganglion demonstrated by restricted lesions of the anteroventral cochlear nucleus. J Comp Neurol. 1992; 320:468–478. [PubMed: 1629399]

Liberman MC. Single-neuron labeling in the cat auditory nerve. Science. 1982; 216:1239–1241. [PubMed: 7079757]

Liu Q, Davis RL. Regional specification of threshold sensitivity and response time in CBA/CaJ mouse spiral ganglion neurons. J Neurophysiol. 2007; 98:2215–2222. [PubMed: 17715200]

Loewenstein WR, Mendelson M. Components of receptor adaptation in a Pacinian corpuscle. J Physiol. 1965; 177:377–397. [PubMed: 14321486]

Lopez CA, Olson ES, Adams JC, Mou K, Denhardt DT, Davis RL. Osteopontin expression detected in adult cochleae and inner ear fluids. Hear Res. 1995; 85:210–222. [PubMed: 7559176]

Lopez I, Ishiyama G, Acuna D, Ishiyama A, Baloh RW. Immunolocalization of voltage-gated calcium channel alpha1 subunits in the chinchilla cochlea. Cell Tissue Res. 2003; 313:177–186. [PubMed: 12845523]

Morris JL, Konig P, Shimizu T, Jobling P, Gibbins IL. Most peptide-containing sensory neurons lack proteins for exocytotic release and vesicular transport of glutamate. J Comp Neurol. 2005; 483:1–16. [PubMed: 15672399]

Mou K, Adamson CL, Davis RL. Time-dependence and cell-type specificity of synergistic neurotrophin actions on spiral ganglion neurons. J Comp Neurol. 1998; 402:129–139. [PubMed: 9831050]

Oertel D. The role of timing in the brain stem auditory nuclei of vertebrates. Annu Rev Physiol. 1999; 61:497–519. [PubMed: 10099699]

Parysek LM, Chisholm RL, Ley CA, Goldman RD. A type III intermediate filament gene is expressed in mature neurons. Neuron. 1988; 1:395–401. [PubMed: 3272173]

Patterson M. Developmental biology. Shaping gradients. Nat Rev Genet. 2001; 2:86–87. [PubMed: 11253057]

Raphael Y, Altschuler RA. Structure and innervation of the cochlea. Brain Res Bull. 2003; 60:397–422. [PubMed: 12787864]

Reichardt LF. Neurotrophin-regulated signalling pathways. Philos Trans R Soc Lond B Biol Sci. 2006; 361:1545–1564. [PubMed: 16939974]

Reid MA, Flores-Otero J, Davis RL. Firing patterns of type II spiral ganglion neurons in vitro. J Neurosci. 2004; 24:733–742. [PubMed: 14736859]

Robles L, Ruggero MA. Mechanics of the mammalian cochlea. Physiol Rev. 2001; 81:1305–1352. [PubMed: 11427697]

Romand R, Sobkowicz H, Emmerling M, Whitlon D, Dahl D. Patterns of neurofilament stain in the spiral ganglion of the developing and adult mouse. Hear Res. 1990; 49:119–125. [PubMed: 1705539]

Rosenblatt KP, Sun ZP, Heller S, Hudspeth AJ. Distribution of Ca^{2+}-activated K^{+} channel isoforms along the tonotopic gradient of the chicken's cochlea. Neuron. 1997; 19:1061–1075. [PubMed: 9390519]

Rubel, EW. Handbook of sensory physiology. Springer-Verlag; Berlin: 1978. Ontogeny of structure and function in the vertebrate auditory system.; p. 135-237.

Rubel EW, Fritzsch B. Auditory system development: primary auditory neurons and their targets. Annu Rev Neurosci. 2002; 25:51–101. [PubMed: 12052904]

Ruben RJ. Development of the mouse: A radioautographic study of terminal mitosis. Acta Otolaryngol. 1967; 220:5–44.

Schimmang T, Tan J, Müller M, Zimmermann U, Rohbock K, Kopschall I, Limberger A, Minichiello L, Knipper M. Lack of Bdnf and TrkB signalling in the postnatal cochlea leads to a spatial reshaping of innervation along the tonotopic axis and hearing loss. Development. 2003; 130:4741–4750. [PubMed: 12925599]

Scroggs RS, Fox AP. Calcium current variation between acutely isolated adult rat dorsal root ganglion neurons. J Physiol. 1992; 445:639–658. [PubMed: 1323671]

Scroggs RS, Todorovic SM, Anderson EG, Fox AP. Variation in I_H, I_{IR}, and I_{Leak} between acutely isolated adult rat dorsal root ganglion neurons of different size. J Neurophysiol. 1994; 71:271–279. [PubMed: 7512627]

Seki M, Nawa H, Fukuchi T, Abe H, Takei N. BDNF is upregulated by postnatal development and visual experience: quantitative and immunohistochemical analyses of BDNF in the rat retina. Invest Ophthalmol Vis Sci. 2003; 44:3211–3218. [PubMed: 12824273]

Sugawara M, Murtie JC, Stankovic KM, Liberman MC, Corfas G. Dynamic patterns of neurotrophin 3 expression in the postnatal mouse inner ear. J Comp Neurol. 2007; 501:30–37. [PubMed: 17206617]

Tabata T. Genetics of morphogen gradients. Nat Rev Genet. 2001; 2:620–630. [PubMed: 11483986]

Tan J, Shepherd RK. Aminoglycoside-induced degeneration of adult spiral ganglion neurons involves differential modulation of tyrosine kinase B and p75 neurotrophin receptor signaling. Am J Pathol. 2006; 169:528–543. [PubMed: 16877354]

Trussell LO. Modulation of transmitter release at giant synapses of the auditory system. Curr Opin Neurobiol. 2002; 12:400–404. [PubMed: 12139987]

Wassle H. Parallel processing in the mammalian retina. Nat Rev Neurosci. 2004; 5:747–757. [PubMed: 15378035]

Wenthold RJ, Yokotani N, Doi K, Wada K. Immunochemical characterization of the non-NMDA glutamate receptor using subunit-specific antibodies. Evidence for a hetero-oli-gomeric structure in rat brain. J Biol Chem. 1992; 267:501–507. [PubMed: 1309749]

Wheeler TC, Chin LS, Li Y, Roudabush FL, Li L. Regulation of synaptophysin degradation by mammalian homologues of seven in absentia. J Biol Chem. 2002; 277:10273–10282. [PubMed: 11786535]

Wiedenmann B, Franke WW. Identification and localization of synaptophysin, an integral membrane glycoprotein of Mr 38,000 characteristic of presynaptic vesicles. Cell. 1985; 41:1017–1028. [PubMed: 3924408]

Yamagata M, Weiner JA, Dulac C, Roth KA, Sanes JR. Labeled lines in the retinotectal system: markers for retinorecipient sublaminae and the retinal ganglion cell subsets that innervate them. Mol Cell Neurosci. 2006; 33:296–310. [PubMed: 16978878]

Zhou Z, Liu Q, Davis RL. Complex regulation of spiral ganglion neuron firing patterns by neurotrophin-3. J Neurosci. 2005; 25:7558–7566. [PubMed: 16107643]

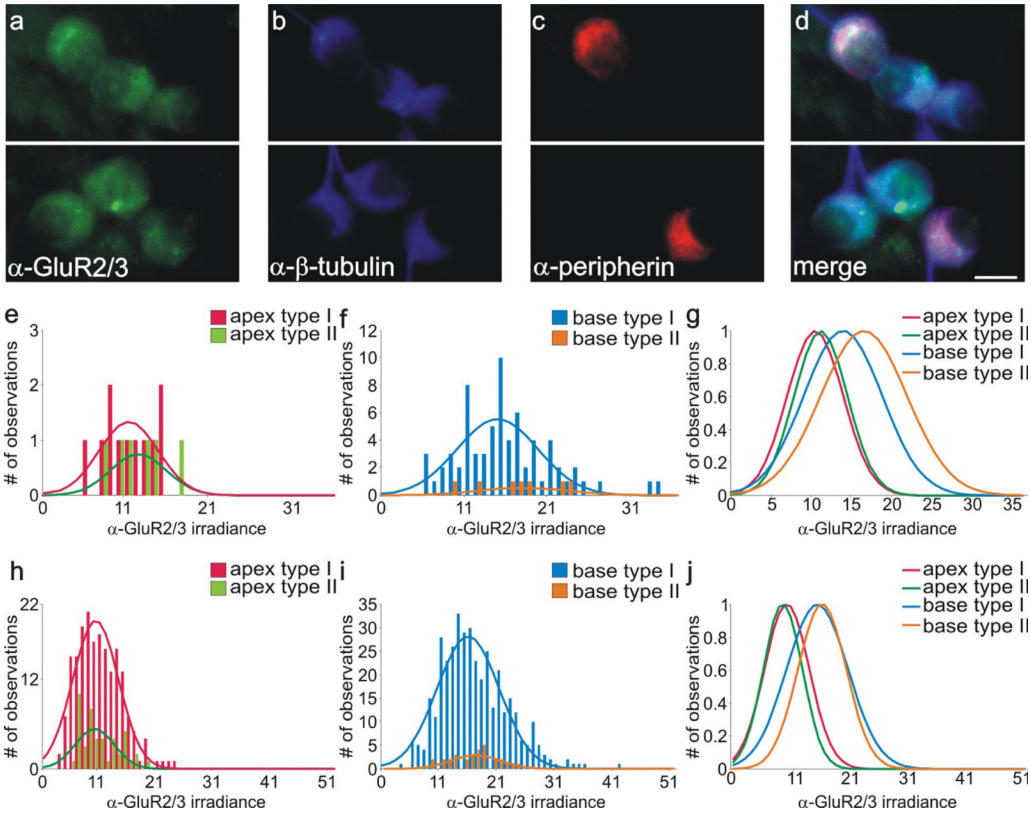

Figure 1.

Type I and type II spiral ganglion neurons in vitro were immunolabeled similarly with anti-GluR2/3 antibody. **a:** Two different fields from the same culture dish show that basal type I and type II spiral ganglion neurons in vitro were comparably stained with anti-GluR2/3 antibody (green). **b:** Both types of spiral ganglion neurons were also stained similarly with anti-β-tubulin antibody (blue). **c:** Anti-peripherin antibody labeling of presumptive type II neurons (red). **d:** Merged image of neurons in a and b show that, although clusters of neurons contained both putative type I and type II neurons, there were no significant differences in their staining patterns with anti-GluR2/3 and anti-β-tubulin antibodies. **e,f:** Frequency histograms of anti-GluR2/3 antibody irradiance measurements from a single experiment; apical type I and type II neurons and basal type I and type II neurons were all well fitted with single Gaussians. **g:** Normalized Gaussian fits for histograms in e and f show that average irradiance levels of both basal type I and type II neurons are greater than those obtained from both classes of apical neuron. **h,i:** Frequency histograms composed of anti-GluR2/3 antibody irradiance measurements from six experiments; apical type I and type II neurons and basal type I and type II neurons were well fitted with single Gaussians. **j:** Normalized Gaussian fits for histograms shown in h and i. Type I and type II distributions were essentially overlapping from each area. As in the single experiment, irradiance levels were consistently highest for both classes of basal neuron. For a magenta-green version see Supporting Information Figure 1. Scale bar = 10 μm.

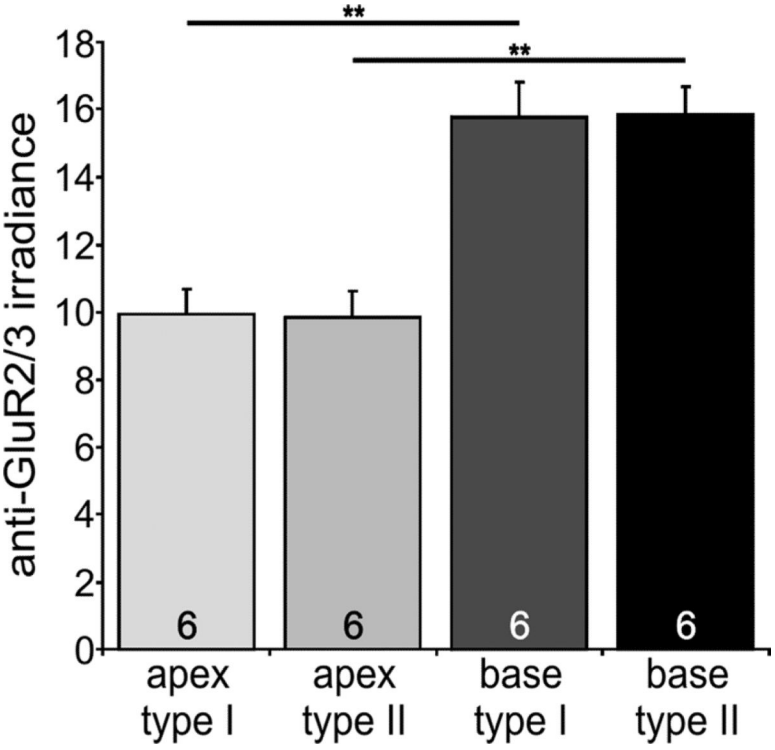

Figure 2.

Quantitative analysis of GluR2/3 enrichment in cultured type I and type II spiral ganglion neurons isolated from the base. An average of six experiments shows that the increased irradiance of basal type I and type II spiral ganglion neurons is statistically significant compared with their apical counterparts. For this figure and subsequent figures, number of experiments is shown in the histogram bars; error bars represent the SEM. Significance of the paired Student's *t*-test, $^{**}P < 0.01$.

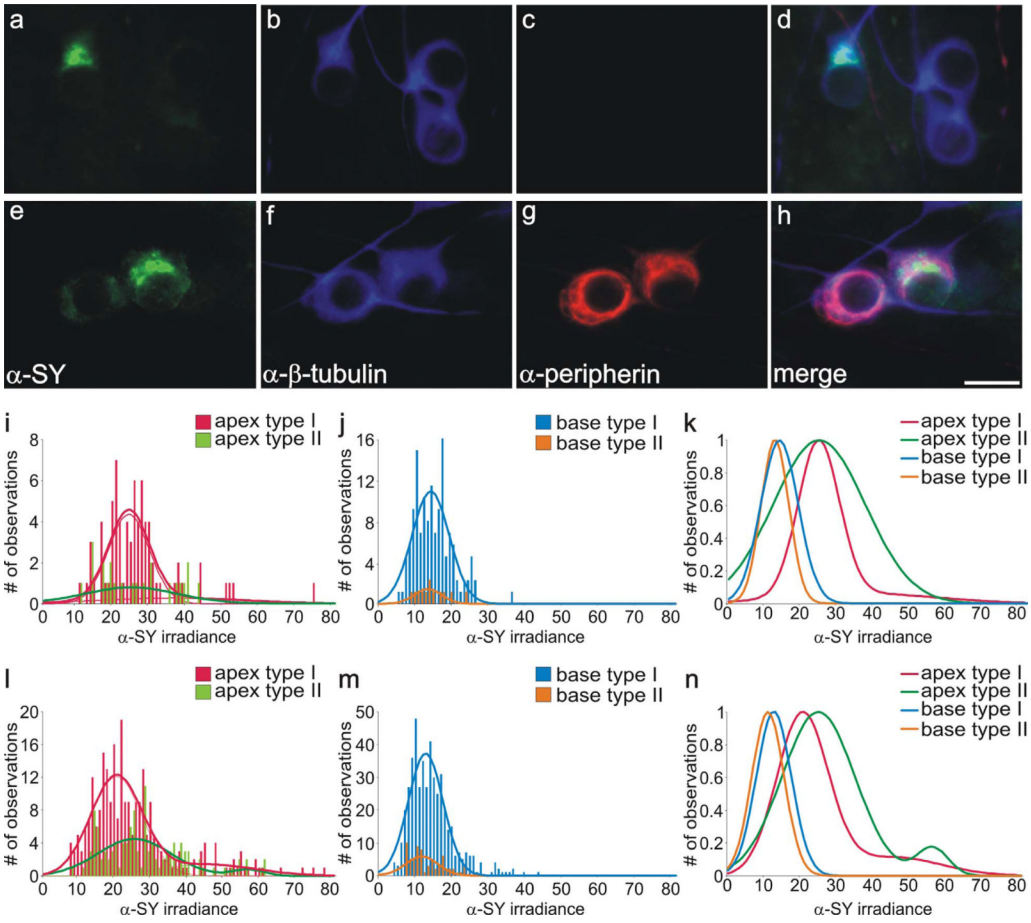

Figure 3.

Type I and type II spiral ganglion neurons isolated in vitro from apical and basal regions showed heterogeneous immunolabeling with anti-synaptophysin antibody. **a–d:** Apical type I spiral ganglion neurons displayed uniform anti-β-tubulin antibody labeling (b, blue) without anti-peripherin antibody labeling (c, red) and showed heterogeneous anti-synaptophysin labeling when viewed alone (a, green) or when a and b were merged (d). **e–h:** Apical type II spiral ganglion neurons displayed uniform anti-β-tubulin labeling (f, blue) with robust anti-peripherin antibody labeling (g, red) and showed heterogeneous anti-synaptophysin labeling when viewed alone (e, green) or when e and f were merged (h). **i,j:** Frequency histograms of anti-synaptophysin antibody irradiance measurements from a single experiment; apical type I and type II neurons and basal type I and type II neurons were all fitted with single Gaussians. **k:** Normalized Gaussian fits for histograms shown in i and j show that average irradiance levels of both apical type I and type II neurons were greater than those obtained from both classes of basal neurons. **l,m:** Frequency histograms composed of anti-synaptophysin antibody irradiance measurements from six experiments; apical type I and type II neurons were well fitted with double Gaussians, and basal type I and type II neurons were well fitted with single Gaussians. **n:** Normalized Gaussian fits for histograms shown in l and m. Within each region, type I and type II distributions were similar, yet irradiance levels of apical neurons were consistently higher than in both classes of basal neuron. For a magenta-green version see Supporting Information Figure 2. Scale bar = 10 μm.

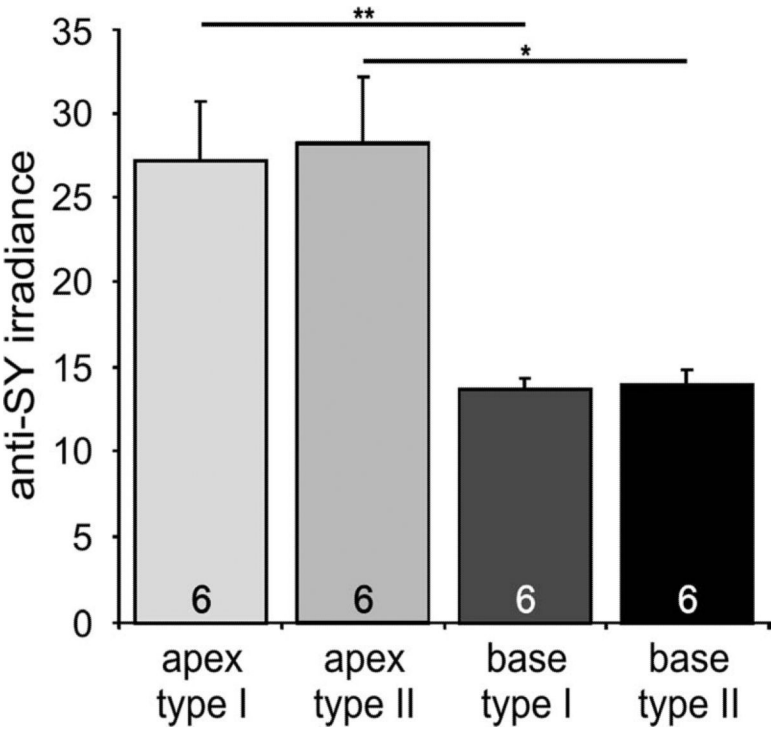

Figure 4.

Synaptophysin is enriched in cultured type I and type II spiral ganglion neurons isolated from the apex. An average of six experiment shows that the increased irradiance of apical type I and type II spiral ganglion neurons is statistically significant compared with their basal counterparts. Significance of the paired Student's *t*-test, $*P < 0.05$; $**P < 0.01$.

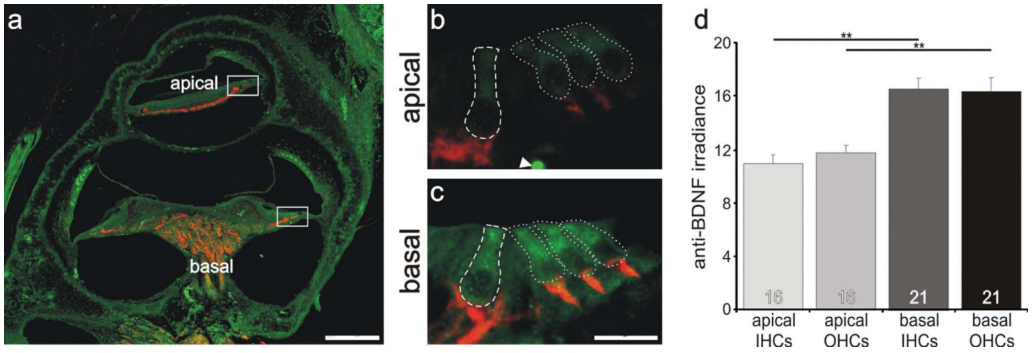

Figure 5.

Inner and outer hair cells located in the basal cochlea had a higher level of anti-BDNF antibody labeling than those located in the apical cochlea. **a:** Low-magnification view of a postnatal tissue section labeled with anti-BDNF (green) and anti-β-tubulin (red) antibodies. **b,c:** High-magnification merged images of sensory hair cells outlined in a (white boxes). Regions of measurement are demarcated with a dashed line for inner hair cells and dotted lines for outer hair cells. **d:** Averages of 15 and 20 measurements (apex and base, respectively) taken from 10 separate sections from three different preparations with two anti-BDNF antibodies showed that irradiance was significantly different between the hair cells from the apical and basal cochlear. Significance of the paired Student's *t*-test, $^{**}P < 0.01$. For a magenta-green version see Supporting Information Figure 3. Scale bars = 120 μm in a; 15 μm in c (applies to b,c).

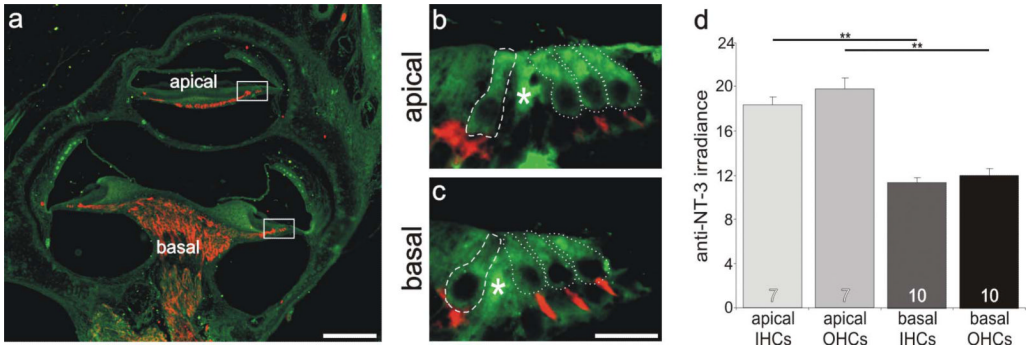

Figure 6.

Inner and outer hair cells located in the apical cochlea had a higher level of anti-NT-3 antibody labeling than those located in the basal cochlea. **a:** Low-magnification view of a postnatal tissue section labeled with anti-NT-3 (green) and anti-β-tubulin (red) antibodies. **b,c:** High-magnification merged images of sensory hair cells outlined in a (white boxes). Regions of measurement are demarcated with a dashed line for inner hair cells and dotted lines for outer hair cells. **d:** Averages of seven and 10 measurements (apex and base, respectively) taken from five separate sections from two different preparations showed that irradiance measurements were significantly different between the hair cells from apical and basal cochlear regions. Significance of the paired Student's *t*-test, $^{**}P < 0.01$. Asterisks indicate areas between inner and outer hair cells that were not measured. For a magenta-green version see Supporting Information Figure 4. Scale bars = 120 μm in a; 15 μm in c (applies to b,c).

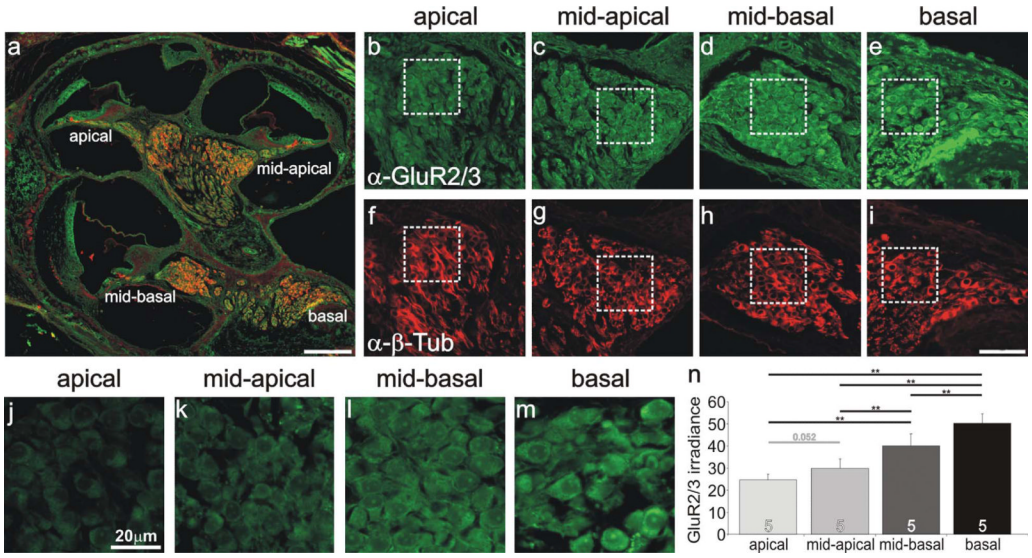

Figure 7.

Anti-GluR2/3 antibody labeling of spiral ganglion neurons was systematically graded along the tonotopic axis. **a:** Low-magnification view of a postnatal cochlear section labeled with anti-GluR2/3 (green) and anti-β-tubulin (red) antibodies, indicating the location of spiral ganglion neurons in different cochlear turns. **b–e:** Anti-GluR2/3 (green) antibody labeling of spiral ganglion neurons was lowest in apical neurons (b), intermediate in midcochlear regions (c,d), and highest in the most basal region (e). **f–i:** Spiral ganglion neurons shown in b–e were uniformly labeled with anti-β-tubulin (red). **j–m:** High-magnification view of neurons outlined with boxes shown in b–e. **n:** Average values from five experiments confirmed that anti-GluR2/3 irradiance levels were highest in basal neurons and decreased systematically in neurons innervating more apical cochlear regions. Significance of the paired Student's *t*-test, $^{**}P < 0.01$. For a magenta-green version see Supporting Information Figure 5. Scale bars = 150 μm in a; 10 μm in i (applies to b–i); 20 μm in j (applies to j–m).

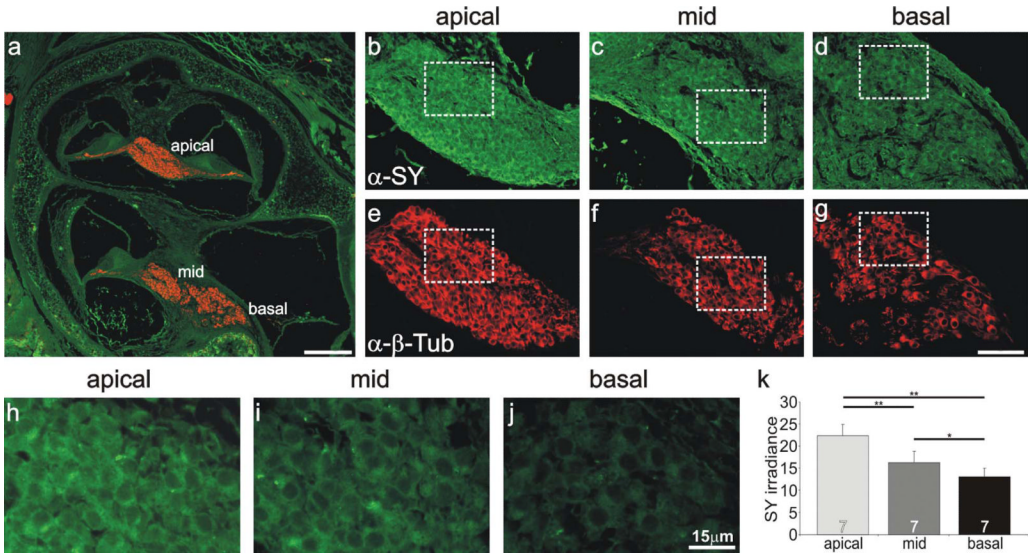

Figure 8.

Anti-synaptophysin antibody labeling of spiral ganglion neurons was systematically graded along the tonotopic axis. **a:** Low-magnification view of a postnatal cochlear section labeled with anti-synaptophysin (green) and anti-β-tubulin (red) indicating the location of spiral ganglion neurons in different cochlear turns. **b–d:** Anti-synaptophysin (green) antibody labeling of spiral ganglion neurons was highest in apical neurons (b), intermediate in a midcochlear region (c), and lowest in the base (d). **e–g:** Spiral ganglion neurons shown from b–d, respectively, were uniformly labeled with anti-β-tubulin (red). **h–j:** High-magnification view of neurons outlined with white boxes shown in b–d. **k:** Average values from seven experiments confirmed that anti-synaptophysin irradiance levels were highest in apical neurons and decreased systematically in neurons innervating more basal cochlear regions. Significance of the paired Student's *t*-test, $*P < 0.05$, $**P < 0.01$. For a magenta-green version see Supporting Information Figure 6. Scale bars = 150 μm in a; 40 μm in g (applies to b–g); 15 μm in j (applies to h–j).

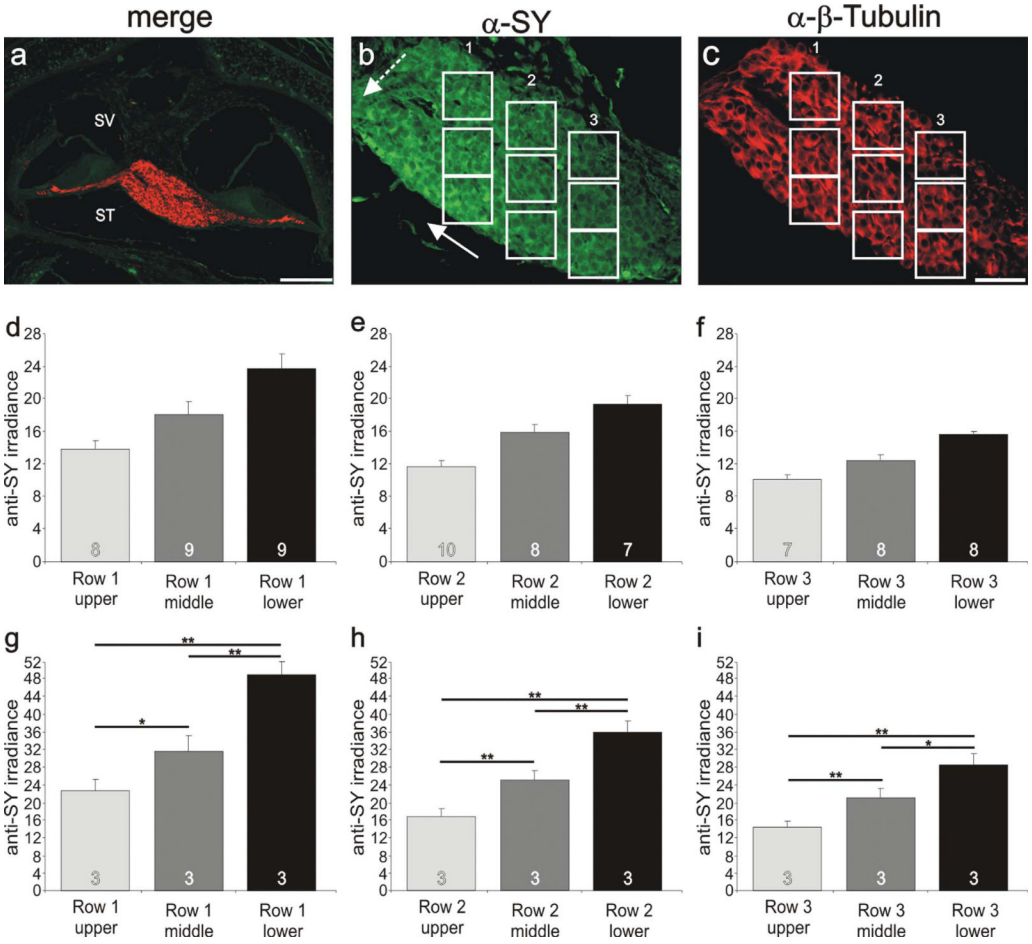

Figure 9.

Local gradients of synaptophysin in postnatal sections are systematically distributed from the scala vestibuli to the scala tympani. **a:** Low-magnification view of a postnatal cochlear section labeled with anti-synaptophysin (green) and anti-β-tubulin (red) antibodies indicating the location of spiral ganglion neurons in an apical cochlear turn. **b:** Anti-synaptophysin (green) antibody labeling of spiral ganglion neurons showed two gradients. The first extends from base to apex (solid arrow); the second extends from scala vestibuli to scala tympani (dashed arrow). Therefore, anti-synaptophysin irradiance was highest in the apical neurons closest to the scala tympani (between the two arrowheads). **c:** Anti-β-tubulin antibody labeling was relatively uniform throughout the region. **d:** Average anti-synaptophysin antibody irradiance measured from neurons within the upper (SV), middle, and lower (ST) regions shown in b, row 1 (white boxes contain 8, 9, and 9 neurons, respectively). **e:** Average anti-synaptophysin antibody irradiance measured from neurons within the upper (SV), middle, and lower (ST) regions shown in b, row 2 (white boxes contain 10, 8, and 7 neurons, respectively). **f:** Average anti-synaptophysin antibody irradiance measured from neurons within the upper (SV), middle, and lower (ST) regions shown in b, row 3 (white boxes contain 7, 8, and 8 neurons, respectively). **g–i:** Average anti-synaptophysin antibody irradiance from three separate experiments measured from neurons within the upper (SV), middle, and lower (ST) regions. g: Row 1 measurements were made from the most apical region within each section. h: Row 2 measurements were made from the midfrequency region within each section. i: Row 3 measurements were made from the most basal region within each section. SV, scala vestibuli; ST, scala tympani. For a

magenta-green version see Supporting Information Figure 7. Significance of the paired Student's *t*-test, **P* < 0.05, ***P* < 0.01. Scale bars = 15 μm in a; 20 μm in c (applies to b,c).

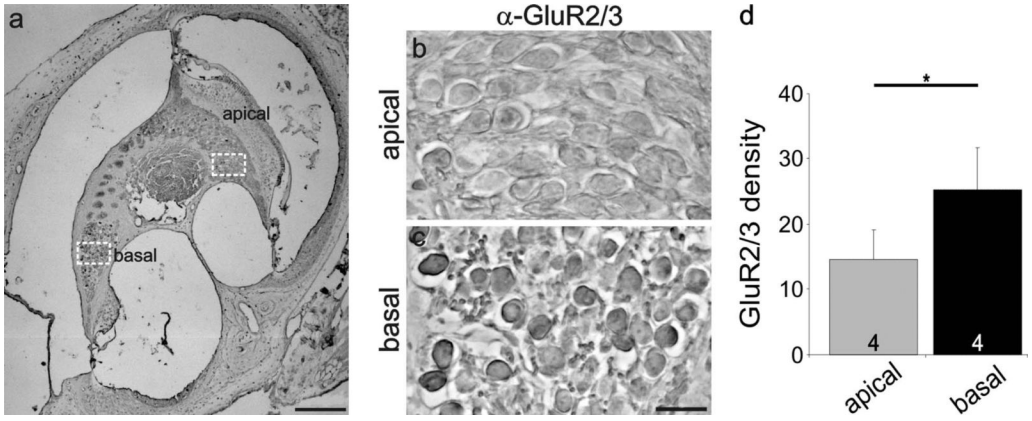

Figure 10.

Differential distribution of anti-GluR2/3 antibody observed postnatally was also present in sections of adult spiral ganglion neurons. **a:** Low-magnification view of an adult cochlear section labeled with anti-GluR2/3 (brown) antibody indicating the location of spiral ganglion neurons in different cochlear turns. **b,c:** High-magnification view of apical and basal neurons (white boxes, a) show higher anti-GluR2/3 antibody density levels in basal neurons (c) compared with apical ones (b). **d:** An average of four experiments confirmed that staining intensity in apical and basal neurons was significantly different. Significance of the paired Student's *t*-test, $*P < 0.05$. Scale bars = 200 μm in a; 20 μm in c (applies to b,c).

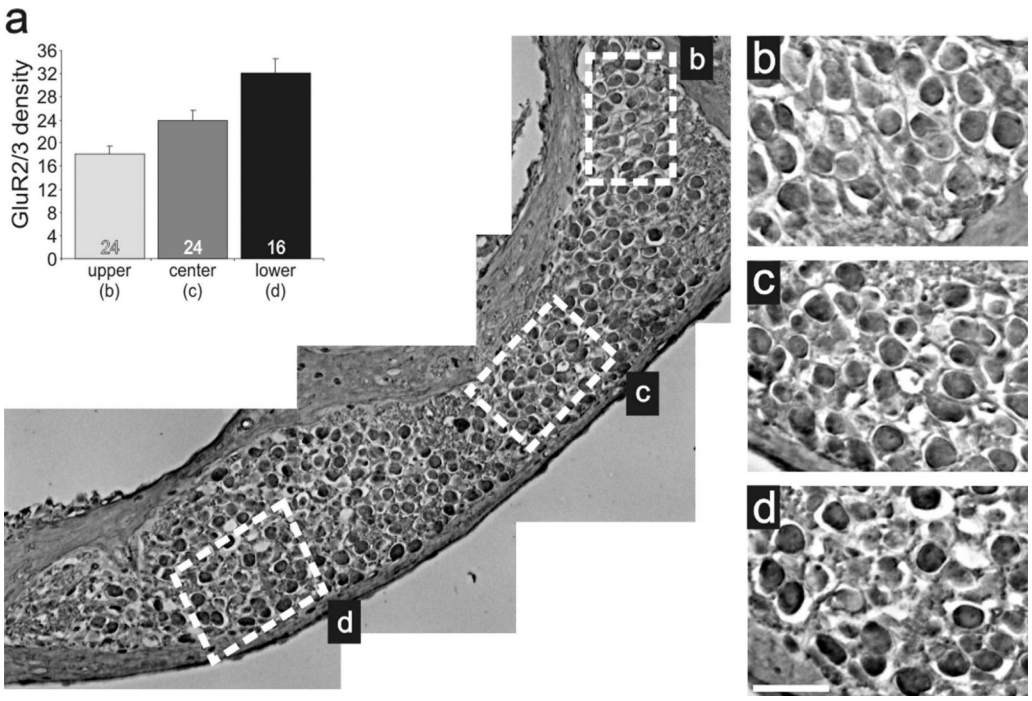

Figure 11.

Anti-GluR2/3 antibody labeling was graded within a localized cochlear region. **a:** Low-magnification image of adult inner ear tissue labeled with anti-GluR2/3 (brown) antibody sectioned to include an elongated region of neurons that spanned the cochlear contour. Average anti-GluR2/3 antibody density levels measured from neurons within the upper (**b**, n = 24), center (**c**, n = 24), and lower (**d**, n = 16) white boxes. b–d. High-magnification images of neurons demarked by white boxes in a showing the subtle increase in anti-GluR2/3 antibody staining intensity in more basal neurons compared with apical ones within a single cochlear turn. The upper region is apical with respect to the lower region. Scale bar = 25 μm in d (applies to b–d).

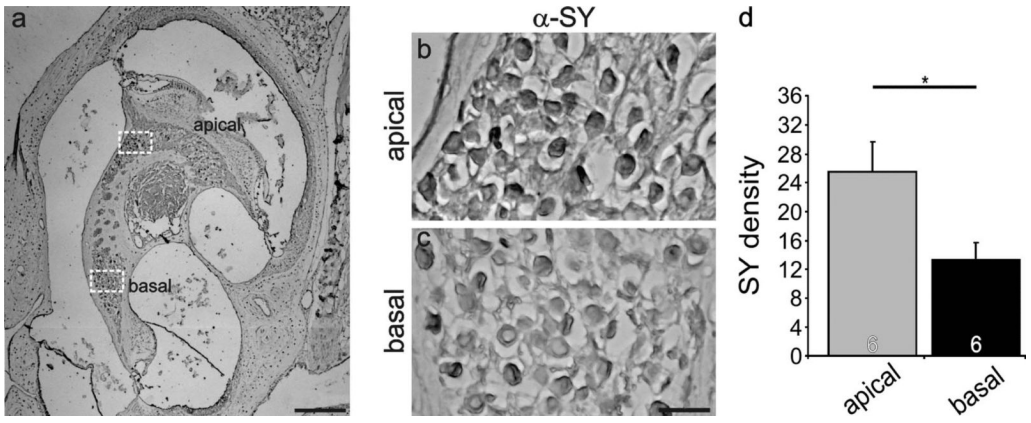

Figure 12.

Differential distribution of anti-synaptophysin antibody observed postnatally was also present in sections of adult spiral ganglion neurons. **a:** Low-magnification view of an adult cochlear section labeled with anti-synaptophysin (brown) antibody indicating the location of spiral ganglion neurons in different cochlear turns. **b,c:** High-magnification view of apical and basal neurons (white boxes, a) illustrating the higher anti-synaptophysin antibody density levels in apical neurons (b) compared with basal ones (c). **d:** An average of six experiments confirmed that staining intensity in apical and basal neurons was significantly different. Significance of the paired Student's *t*-test, $*P < 0.05$. Scale bars = 200 μm in a; 20 μm in c (applies to b,c).

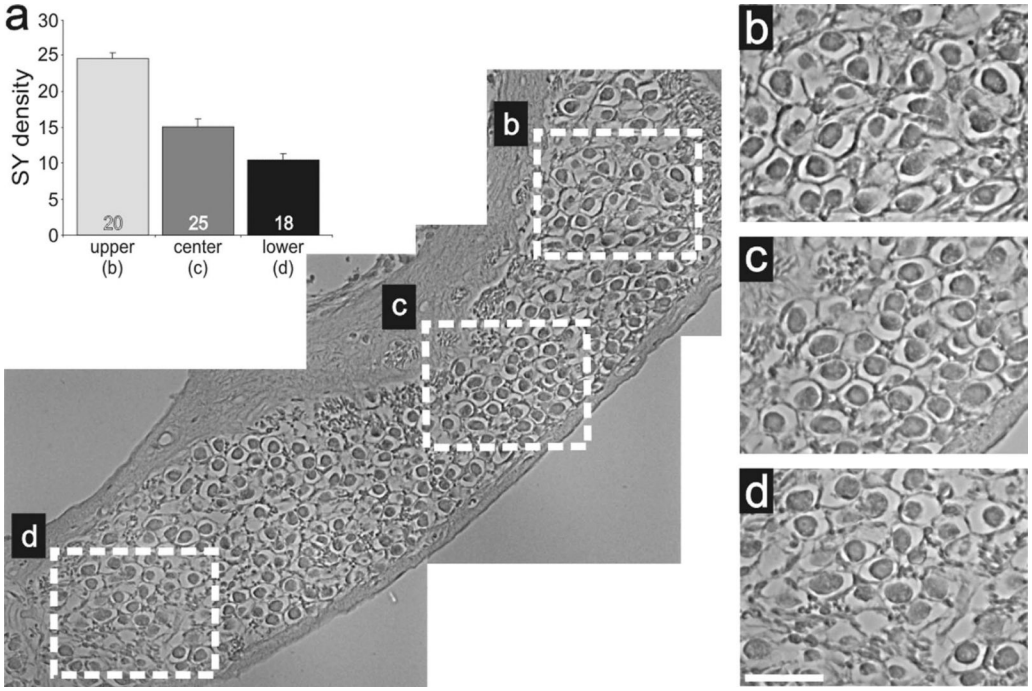

Figure 13.

Anti-synaptophysin antibody labeling was graded within a localized cochlear region. **a:** Low-magnification image of adult inner ear tissue labeled with anti-GluR2/3 (brown) antibody sectioned to include an elongated region of neurons that spanned the cochlear contour. **Inset:** Average anti-synaptophysin antibody density levels measured from neurons within the upper (**b**, n = 20), center (**c**, n = 25), and lower (**d**, n = 18) white boxes. b–d: High-magnification images of neurons demarked by white boxes in a showing the subtle increase in anti-synaptophysin antibody staining intensity in more apical neurons compared with basal ones within a single cochlear turn. Scale bar = 25 μm in d (applies to b–d).

TABLE I

Primary Antibodies

Antigen	Immunogen	Manufacturer	Dilution
GluR2/3	Amino acids 850–862 EGYNVYGIESVKI	Chemicon, AB1506, polyclonal, raised in rabbit, affinity purified	1:100
Synaptophysin	Synaptosome preparation from rat retina	Sigma-Aldrich, S5768, clone SVP-38, monoclonal, raised in mouse, mouse IgG1 isotype	1:50
BDNF (1)	Epitope mapping within an internal region of BDNF of human origin; amino acids 128–147	Santa Cruz Biotechnology, N-20, sc-546, polyclonal, raised in rabbit	1:100
BDNF (2)	Recombinant full-length protein (human)	Abcam, ab6201, polyclonal, raised in rabbit	1:200
NT-3	11-Amino-acid peptide (YAEHKSHRGEY) corresponding to the amino acid-terminal of mouse NT-3 coupled to BSA	Millipore, AB1527, polyclonal, raised in sheep	1:100
Tubulin	Microtubule derived from rat brain, reactive to neuron specific class III β-tubulin	Covance, PRB-435P, polyclonal, raised in rabbit	1:200
Tubulin (TUJ1)	Microtubule derived from rat brain, reactive to neuron specific class III β-tubulin	Covance, MMS-435P, monoclonal, raised in mouse	1:200
Peripherin	Electrophoretically pure trp-E-peripherin fusion protein containing all but the four N-terminal amino acids of rat peripherin	Chemicon, AB-1530, polyclonal, raised in rabbit	1:4,000
Peripherin	Electrophoretically pure trp-E-peripherin fusion protein containing all but the four N-terminal amino acids of rat peripherin	Chemicon, MAB-1527, monoclonal, raised in mouse	1:4,000